

Identifying Unmeasured Confounders in Panel Causal Models: A Two-Stage LM-Wald Approach

Bang Quan Zheng
University of Texas at Austin
bangquan@ucla.edu

Abstract

Panel data are widely used in political science to draw causal inferences. However, these models often rely on the strong and untested assumption of sequential ignorability—that no unmeasured variables influence both the independent and outcome variables across time. Grounded in psychometric literature on latent variable modeling, this paper introduces the Two-Stage LM-Wald (2SLW) approach, a diagnostic tool that extends the Lagrange Multiplier (LM) and Wald tests to detect violations of this assumption in panel causal models. Using Monte Carlo simulations within the Random Intercept Cross-Lagged Panel Model (RI-CLPM), which separates within- and between-person effects, I demonstrate the 2SLW’s ability to detect unmeasured confounding across three key scenarios: biased correlations, distorted direct effects, and altered mediation pathways. I also illustrate the approach with an empirical application to real-world panel data. By providing a practical and theoretically grounded diagnostic, the 2SLW approach enhances the robustness of causal inferences in the presence of potential time-varying confounders. Moreover, it can be readily implemented using the R package `lavaan`.

Keywords: Panel causal model, RI-CLPM, unmeasured confounding, sensitivity analysis

1 Introduction

In recent decades, political scientists have increasingly focused on the methodological challenges of identifying causal mechanisms, often turning to longitudinal panel data analyzed through approaches such as cross-lagged panel models (CLPMs), latent growth curve models, and random intercept cross-lagged panel models (RI-CLPMs). In line with this trend, researchers have adopted structural equation modeling (SEM) with latent variables to measure unobserved constructs and uncover underlying causal pathways—particularly when experimental designs are impractical (Chiu, Lan, Liu, & Xu, 2025). For example, scholars have examined causal relationships using panel data such as those between partisanship and core values (Goren, 2005) and between authoritarianism and Republican support (Luttig, 2021), personality and political preferences (Bakker, Schumacher, & Rooduijn, 2021), the ideological roots of moral intuition (Hatemi, Crabtree, & Smith, 2019), and the effects of political trust on social trust over time (Dinesen, Sonderskov, Sohlberg, & Esaiasson, 2022). These examples reflect a broader wave of research that uses panel data to uncover the dynamics of political attitudes and behavior. Unmeasured confounding in panel models poses a persistent challenge, however, with significant implications for both theoretical understanding and policy formulation. Current methods often fail to adequately address this issue.

While panel analyses offer valuable leverage for identifying causal relationships, they rely on a critical assumption: sequential ignorability—the idea that no unmeasured factors influence both the independent and outcome variables across waves. When this assumption is violated, unmeasured confounding can introduce spurious associations, distorting causal estimates and masking true underlying mechanisms. Sensitivity analysis is essential for assessing how unmeasured confounding may bias results (Acharya, Blackwell, & Sen, 2016; Blackwell, 2014; Imai, Keele, & Tingley, 2010; Imai, Keele, Tingley, & Yamada, 2011; Imai & Yamamoto, 2013), but existing methods are limited for panel models with multiple waves and complex interdependencies. They typically examine one independent variable at a time and often fail to account for latent residual correlations or unmeasured confounders that may

influence multiple pathways simultaneously (Harring, McNeish, & Hancock, 2017). Manual variable selection in sensitivity analysis introduces subjectivity, reducing reliability and limiting the detection of confounders (Blackwell, 2014).

Moreover, prior research shows that complex models—with more parameters, limited sample sizes, and intricate temporal structures—are especially prone to specification errors, including overlooked confounders (Zheng & Bentler, 2025). This issue is particularly acute in multi-wave panel models that include autoregressive (AR) and cross-lagged (CL) effects, where stable individual differences, if uncontrolled, can bias estimates of within-person dynamics (Feldman, Panish, Weber, & Zheng, 2025). As scholars have noted, analytic models in this area often overestimate causal effects (Bakker et al., 2021; Lucas, 2023). Such biases can carry significant theoretical and policy implications.

To address these challenges, this study builds on the ‘improved LM test’ proposed by Zheng and Bentler (2025) and introduces a two-stage sequential approach that combines the strengths of the Lagrange Multiplier (LM) test and the Wald test to detect potential confounders in panel causal models. I term this the Two-Stage LM-Wald (2SLW) approach—a data-driven method for detecting both observed and unobserved confounders, identifying path misspecifications and unmeasured confounders in SEM-based panel models, and evaluating the influence of latent and observed variables while accounting for measurement error. Drawing on psychometric literature, the proposed approach first applies the LM test to detect potential unmeasured confounders, and then uses the Wald test to identify which specific cross-lagged or autoregressive paths are affected. More importantly, the 2SLW method simultaneously diagnoses model misspecification and unmeasured confounding. It is applicable to both continuous and discrete variables and is designed for parametric models.

I demonstrate the 2SLW approach using RI-CLPMs, which preserve the core dynamics of CLPMs while separating stable between-person differences from within-person changes, providing a more general framework for specification diagnostics. Monte Carlo simulations show that 2SLW effectively detects unmeasured confounders in three common situations:

when a hidden factor biases the relationship between the independent and outcome variables, distorts a mediation pathway, or alters a direct effect. I also apply the method to real panel data with discrete variables measured across three waves, further illustrating its practical usefulness. While this paper focuses on demonstrating 2SLW within the RI-CLPM, the method is also applicable to other longitudinal panel models, such as second-order RI-CLPM and standard CLPM (see the Appendix). Importantly, the 2SLW procedure can be readily implemented using the widely used R package `lavaan` making it accessible to applied researchers.

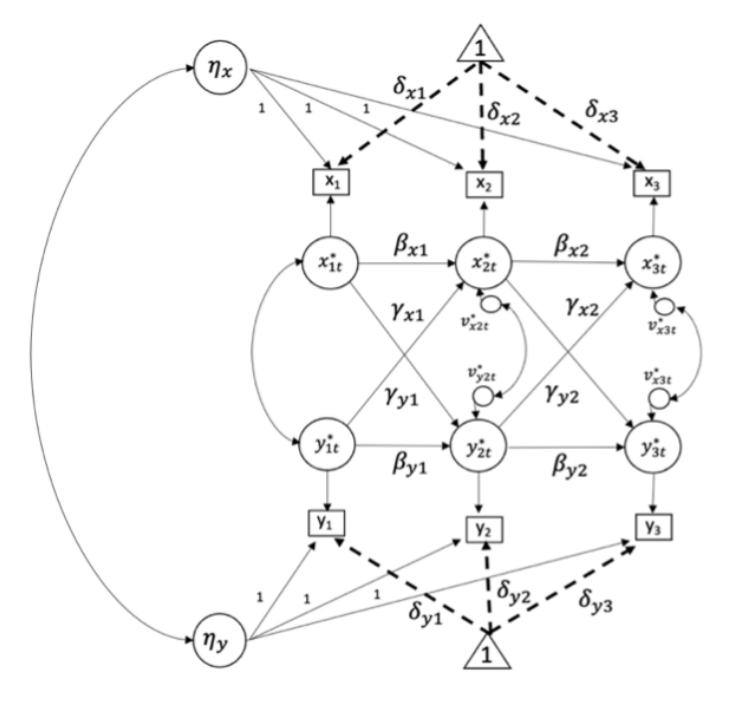
This paper proceeds as follows: Section 2 reviews the RI-CLPM in panel causal inference. Section 3 discusses challenges in conventional sensitivity analysis for panel models. Section 4 reviews the LM and Wald tests. Section 5 introduces the simulation setup, followed by simulation results in Section 6. Section 7 presents an empirical illustration. Finally, Section 8 offers discussion and conclusions.

2 RI-CLPM for Panel Causal Inference

The RI-CLPM has become a widely used method for analyzing causal relationships in longitudinal data in the social and behavioral sciences. It extends the traditional CLPM framework by addressing a key limitation: the conflation of between-person differences with within-person changes. By separating stable between-person differences from within-person dynamics, the RI-CLPM helps correct for bias introduced by time-invariant confounders—a core weakness of standard CLPMs (Hamaker, Kuiper, & Grasman, 2015; Usami, Murayama, & Hamaker, 2019). This distinction helps correct for bias that arises when time-invariant confounders are ignored—a major limitation of standard CLPMs (Lucas, 2023). The CLPM assumes that all relevant stable traits are either measured or irrelevant. When this assumption is violated, unobserved stable factors can confound the cross-lagged estimates. Although the RI-CLPM captures stable between-person variance through random intercepts, it is still

vulnerable to time-varying unmeasured confounders. Additionally, in standard CLPMs, unaccounted measurement error can distort AR and CL estimates, leading to misleading conclusions about within-person stability and change (Feldman et al., 2025; Hamaker et al., 2015; Lucas, 2023; Mund, Johnson, & Nestler, 2021).

Figure 1: Diagram of RI-CLPM



As Figure 1 illustrates, RI-CLPMs help identify the causal direction and strength of relationships by examining how one variable at an earlier time point predicts another at a later time point in multi-wave panel data, while controlling for prior levels of both variables and separating stable between-person differences from within-person fluctuations, which makes it easier to isolate the dynamic causal mechanisms at play. For statistical illustration, I consider a simple bivariate model. Suppose we are interested in examining the temporal reciprocal relationships between two random variables, x_i and y_i . Also, I use x_{it} and y_{it} to denote the measurements at time point t for individual i ($i = 1, \dots, n; t = 1, \dots, T$). The RI-CLPM can be expressed as follows:

$$x_{it} = \delta_{xt} + \eta_{xi} + x_{it}^*, \quad (1)$$

$$y_{it} = \delta_{yt} + \eta_{yi} + y_{it}^*. \quad (2)$$

Here, δ_{xt} and δ_{yt} represent temporal group means at time point t , and η_{xi} and η_{yi} are individual-level time-invariant trait factors. In the RI-CLPM, δ_{xt} and δ_{yt} aim to capture mean growth trajectories, and x_{it}^* and y_{it}^* are temporal deviation terms, which capture the temporal within-person deviations from the means of each person i . As such, we need to partition the between-person level and within-person level to understand the dynamics between the effect of time-invariant stable trait factors and time-varying occasion-specific factors. In the context of Equations (1) and (2), x_{it}^* and y_{it}^* capture the temporal deviations from the expected values of x_{it} and y_{it} , that is, $\delta_{xt} + \eta_{xi}$ and $\delta_{yt} + \eta_{yi}$. Thus, the within-person reciprocal relations are modeled using lagged effects and temporal trait factors (Hamaker et al., 2015; Usami, 2021). The within-person reciprocal relations are defined as:

$$x_{it}^* = \beta_x x_{i(t-1)}^* + \gamma_x y_{i(t-1)}^* + v_{xit}, \quad (3)$$

$$y_{it}^* = \beta_y y_{i(t-1)}^* + \gamma_y x_{i(t-1)}^* + v_{yit}, \quad (4)$$

where β_x and β_y are AR parameters that measure the within-person stability of x and y , respectively. γ_x and γ_y are CL parameters that capture reciprocal relations between x and y . v_{xit} and v_{yit} are the residuals, which are assumed to follow a normal distribution with an unknown variance $N(0, \sigma^2)$.

$$\begin{bmatrix} x_{it} \\ y_{it} \end{bmatrix} = \begin{bmatrix} \delta_{xt} \\ \delta_{yt} \end{bmatrix} + \begin{bmatrix} \eta_{xi} \\ \eta_{yi} \end{bmatrix} + \begin{bmatrix} \beta_x & \gamma_x \\ \beta_y & \gamma_y \end{bmatrix} \begin{bmatrix} x_{i(t-1)}^* \\ y_{i(t-1)}^* \end{bmatrix} + \begin{bmatrix} v_{xit} \\ v_{yit} \end{bmatrix}. \quad (5)$$

It is important to note that β_x and β_y do not necessarily represent the stability of the

rank order of individuals from one occasion to another; instead, they indicate the magnitude of within-person carry-over effect (Hamaker et al., 2015). However, their residuals may share common variance, which can be expressed as:

$$\rho = \text{Cor}(v_{xit}, v_{yit}), \tag{6}$$

where ρ denotes the correlation between v_{xit} and v_{yit} . The sequential ignorability assumes $v_{xit} \perp v_{yit}$, implying $\rho = 0$. If $\rho \neq 0$, it indicates the presence of an unmeasured confounder affecting both the independent and outcome variables.

Although RI-CLPM addresses stable, trait-level confounders, it cannot account for unobserved confounders that vary over time or for concurrent effects, both of which can bias within-person estimates. Incorporating observed time-varying confounders and examining concurrent structures can improve validity. When an unmeasured latent variable influences both independent and outcome variables—or multiple variables within a cross-lagged structure—it violates sequential ignorability and can bias results through shared variance (Lucas, 2023). Misattributing shared variance to specified paths rather than omitted confounders can bias coefficients—potentially inflating, weakening, or reversing their sign—so that even small unaccounted influences may distort causal interpretation. In addition, if factor loadings are weak, the latent variables are poorly measured, which makes the estimated cross-lagged paths unstable. Conversely, if factor loadings are too strong, say, close to 1, the latent construct overlaps almost completely with the observed measure, leading to identification problems and suppressing meaningful variance that would otherwise inform cross-lagged relations (see the Appendix for details).

2.1 Key Differences between CFA and RI-CLPM

This study adapts the joint LM and Wald tests—introduced by Zheng and Bentler (2025) for use in Confirmatory Factor Analysis (CFA)—to the context of panel causal models,

where their application presents important methodological distinctions. While the statistical foundations of these tests remain consistent, several key differences between CFA and RI-CLPMs warrant careful attention.

First, CFA assumes a stationary structure with stable loadings and residuals, whereas RI-CLPM models dynamic processes over time. RI-CLPM introduces random intercepts and time-ordered constraints, increasing complexity and limiting the flexibility of the covariance structure. Consequently, LM test statistics in RI-CLPMs may appear inflated or misleading due to misspecification or convergence issues.

Second, LM tests in CFA typically identify local misfit (e.g., residual correlations) under the assumption of local independence. In contrast, RI-CLPM's temporal interdependence and feedback loops complicate such diagnostics. LM tests in this context often fail to detect dynamic interactions or suppressor effects, leading to potentially misleading modification suggestions.

Third, panel model misfit is often global—arising from violations of stationarity, measurement invariance, or residual autocorrelation—that LM tests may overlook. In addition, the random intercepts in RI-CLPMs absorb between-person variance, which can mask within-person misspecifications, while measurement error may further weaken test power, leading to false negatives or overfitting through theoretically inconsistent paths (Zheng & Valente, 2023).

In sum, although the LM test framework can be extended to RI-CLPMs, its application is far from straightforward. The dynamic, multilevel nature of panel models requires careful interpretation of results and underscores the need for diagnostic tools specifically designed for longitudinal causal inference. Given their sensitivity to model structure, misspecification, and latent confounding, more robust, tailored diagnostics are essential.

3 Challenges in Sensitivity Analysis & Proposed Research Strategy

Sensitivity analysis plays a crucial role in evaluating the robustness of causal conclusions, particularly in the presence of potential unmeasured confounders. While political methodologists have developed formal tools for sensitivity analysis (Acharya et al., 2016; Blackwell, 2014; Imai et al., 2010, 2011), these methods do not readily extend to complex longitudinal models such as the RI-CLPM or other panel causal models. In these settings, confounding is more nuanced: time-invariant and time-varying unobserved factors may influence multiple variables across waves, introducing bias even when initial exposures are randomized.

However, in panel models like the RI-CLPM—which include reciprocal relationships, repeated measurements, and latent constructs—the potential for unmeasured confounding is both more complex and harder to detect. Time-invariant confounders open multiple backdoor paths, introducing bias into the estimated causal effects. That is, confounders may simultaneously affect multiple variables across time, not just the residuals of mediator and outcome. Moreover, traditional sensitivity analyses designed for static models are not well-suited to detect the broader model misfit that arises when these confounding structures are present.

A persistent challenge in panel causal analysis with intermediate or time-varying variables is that, even when the initial exposure is randomized, subsequent variables—such as mediators, attitudes, or behaviors—may still be endogenous. These variables may be influenced by stable traits, prior experiences, or other latent factors, which also affect downstream outcomes. For example, in studies of immigration attitudes, both media exposure and policy preferences may be shaped by underlying ideological dispositions or ethnocentric orientations that are rarely measured directly. As a result, estimates of causal effects may conflate genuine relationships with spurious associations caused by unmeasured confounders or self-selection processes. This issue is particularly acute in dynamic models where feedback loops

and reciprocal causation are possible (Bullock, Green, & Ha, 2010; Holland, 1988; Imai et al., 2011; MacKinnon, 2008; MacKinnon & Pirlott, 2015; Pearl, 2001; Robins & Greenland, 1992). To address these challenges, researchers need diagnostic tools capable of assessing model specification and detecting unaccounted confounding pathways—particularly in longitudinal SEMs. The 2SLW approach introduced in this paper offers a novel method for identifying unmeasured confounding in RI-CLPMs and for model specification search.

3.1 Research Strategy

The illustration of the 2SLW method proceeds in three steps. First, I generate data from a population RI-CLPM that includes omitted unmeasured confounders, then fit an analysis model that excludes them—mimicking the misspecifications researchers might make in practice. This deliberate violation of the sequential ignorability assumption ensures poor model fit, creating conditions to detect misspecifications.

Second, I apply a univariate LM test to identify the top 25 candidate parameters ranked by LM χ^2 statistics and Expected Parameter Change (EPC) values, excluding those with small EPCs, violations of temporal ordering, or potential non-identification problems in the RI-CLPM.

Third, I refine the model using a forward stepwise Wald test, retaining only parameters with $p < 0.05$ while removing any that cause convergence issues, non-positive definite covariance matrices, or negative variances. Identified parameters suggest possible unmeasured confounders, which I incorporate into an extended RI-CLPM to assess their effect on autoregressive and cross-lagged coefficients. Substantial changes imply bias from unmeasured confounding, whereas stability increases confidence in the model’s robustness.

This procedure—combining LM-driven detection with Wald-based parsimony—offers a structured, scalable approach to sensitivity analysis for SEM-based panel models and can be implemented in R using `lavaan`.

4 LM Test & Wald Test

This section reviews the statistical foundations of the 2SLW approach. The LM test is a widely used diagnostic tool in SEM to assess whether freeing constrained parameters would improve model fit—often used to detect potential omitted paths. Formally, given a model with q free parameters and r constraints ($r < q$), the LM statistic evaluates whether any constrained parameters should be freed. When variables are continuous and normally distributed, the LM statistic is derived from the maximum likelihood fit function:

$$F(\boldsymbol{\theta}) = \log |\boldsymbol{\Sigma}(\boldsymbol{\theta})| - \log |\mathbf{S}| + \text{tr}(\mathbf{S} \boldsymbol{\Sigma}(\boldsymbol{\theta})^{-1}) - p \quad (7)$$

Let $\hat{\boldsymbol{\theta}}$ is a vector of constrained estimators of $\boldsymbol{\theta}$ subject to constraints $\mathbf{h}(\boldsymbol{\theta}) = 0$. With r constraints, there exists an $r \times 1$ constraint vector $\mathbf{h}(\boldsymbol{\theta})' = (h_1, \dots, h_r)$. When minimizing the fit function $F(\boldsymbol{\theta})$ subject to $\mathbf{h}(\boldsymbol{\theta}) = 0$, matrices of derivatives $\mathbf{g} = \frac{\partial F}{\partial \boldsymbol{\theta}}$ and $\mathbf{L}' = \frac{\partial \mathbf{h}}{\partial \boldsymbol{\theta}}$ exist, and a vector of Lagrange multipliers $\hat{\boldsymbol{\lambda}}$ can be defined such that:

$$\hat{\mathbf{g}} + \hat{\mathbf{L}}' \hat{\boldsymbol{\lambda}} = 0 \quad \text{and} \quad \mathbf{h}(\hat{\boldsymbol{\theta}}) = 0. \quad (8)$$

In the context of constraints, the asymptotic covariance matrix can be derived from a matrix based on \mathbf{H} , augmented by the matrix of derivatives \mathbf{L} and a null matrix \mathbf{O} . The sample variance-covariance matrix of the estimated parameter $\sqrt{n}(\hat{\boldsymbol{\theta}} - \boldsymbol{\theta})$ is given by the inverse of the information matrix $\mathbf{H}(\boldsymbol{\theta})$ in the case of maximum likelihood estimation, and \mathbf{R} gives the covariance matrix of the Lagrange multipliers $\sqrt{n}(\hat{\boldsymbol{\lambda}} - \boldsymbol{\lambda})$, which is derived from the inverse of the information matrix \mathbf{L} . Hence, we can define:

$$\begin{bmatrix} \mathbf{H} & \mathbf{L}' \\ \mathbf{L} & \mathbf{O} \end{bmatrix}^{-1} = \begin{bmatrix} \mathbf{H}^{-1} - \mathbf{H}^{-1} \mathbf{L}' (\mathbf{L} \mathbf{H}^{-1} \mathbf{L}')^{-1} & \mathbf{H}^{-1} \mathbf{L}' (\mathbf{L} \mathbf{H}^{-1} \mathbf{L}')^{-1} \\ (\mathbf{L} \mathbf{H}^{-1} \mathbf{L}')^{-1} \mathbf{L} \mathbf{H}^{-1} & -(\mathbf{L} \mathbf{H}^{-1} \mathbf{L}')^{-1} \end{bmatrix} = \begin{bmatrix} \mathbf{M} & \mathbf{T}' \\ \mathbf{T} & -\mathbf{R} \end{bmatrix}. \quad (9)$$

Under regularity conditions and the null hypothesis $H(\theta)$, the LM test statistic is asymptotically distributed as a χ^2 variate with r degrees of freedom. When testing a single constraint, the univariate LM statistic follows a χ^2 variate with 1 degree of freedom. This makes the test particularly useful for evaluating whether a specific parameter in the θ_r vector is equal to 0:

$$T_{LMi} = n \hat{\lambda}_i^2 \hat{\mathbf{R}}_{ii}^{-1} \hat{\lambda}_i \sim \chi_{r1}^2. \quad (10)$$

4.1 Expected Parameter Change (EPC)

The LM test provides the expected parameter change (EPC) score, which estimates how much a fixed or constrained parameter would shift if freely estimated. Researchers commonly use the LM test with EPCs to identify potential model modifications and unmeasured confounders in SEM. Oberski (2014), for instance, used EPC to evaluate the sensitivity of substantive parameters to violations of measurement invariance. The EPC approximates the expected change in parameters of interest when cross-group invariance constraints are relaxed, demonstrating how unaccounted measurement differences could confound substantive conclusions.

In this study, I use EPCs as a form of local sensitivity analysis to examine whether fixed structural paths significantly influence model estimates. Based on the statistical framework of the LM test in Equation (10), the univariate EPC for a fixed parameter can be expressed as

$$\text{EPC}_i = \frac{\hat{\lambda}_i}{\hat{\mathbf{R}}_{ii}}. \quad (11)$$

The subscript indicates evaluation at the constrained estimate. While a particular parameter may change when the constraint is released, its effects can be assessed across all constraint equations to identify which constraints may be worth relaxing (Chou & Bentler,

1993). Large EPCs indicate potential overconstraints in the model.

This issue is especially pronounced with small samples, where the LM test’s effectiveness is diminished and more vulnerable to random fluctuations (MacCallum, Roznowski, & Nectowitz, 1992; Yuan & Liu, 2021). Moreover, LM test performance is shaped by sample size, degrees of freedom (df), and model complexity. The LM test assesses all possible paths based on the model’s df; while more df raise the risk of detecting spurious paths—especially when few are truly omitted—this risk decreases with larger sample sizes (Zheng & Bentler, 2025).

4.2 The Wald Test

The Wald test statistic complements the LM test and is calculated as follows:

$$W = n \hat{\boldsymbol{\theta}}_r' (\hat{\mathbf{L}} \hat{\mathbf{H}}^{-1} \hat{\mathbf{L}}') \hat{\boldsymbol{\theta}}_r \sim \chi_r^2, \quad (12)$$

where $\hat{\mathbf{L}}$ is a matrix defining the constraints. Larger values indicate stronger evidence against the null. The univariate Wald statistic for each parameter in $\hat{\boldsymbol{\theta}}_r$ can be computed as

$$W_i = n \hat{\boldsymbol{\theta}}_i \hat{\mathbf{H}}_{ii}^{-1}, \quad \hat{\boldsymbol{\theta}}_i = \frac{n \hat{\boldsymbol{\theta}}_i^2}{\hat{\mathbf{H}}_{ii}} \sim \chi_1^2, \quad (13)$$

where $\hat{\boldsymbol{\theta}}_i$ is one of the parameters in $\hat{\boldsymbol{\theta}}_r$ and $\hat{\mathbf{H}}_{ii}$ is the i th diagonal element of the information matrix $\hat{\mathbf{H}}$. The Wald test often uses a stepwise procedure: parameters with $p < 0.05$ are retained, and the process continues until all have been evaluated.

5 Monte Carlo Simulation

This simulation study involves three main steps. In the first step, I generate simulated data from three distinct RI-CLPMs, which serve as our population models. The data generation follows the RI-CLPM covariance matrix structure (see Appendix). Specifically, a

p -dimensional variable, \mathbf{z}_i , is generated as

$$\mathbf{z}_i = \boldsymbol{\Sigma}(\boldsymbol{\theta})^{1/2} \boldsymbol{\varepsilon}_i, \quad (14)$$

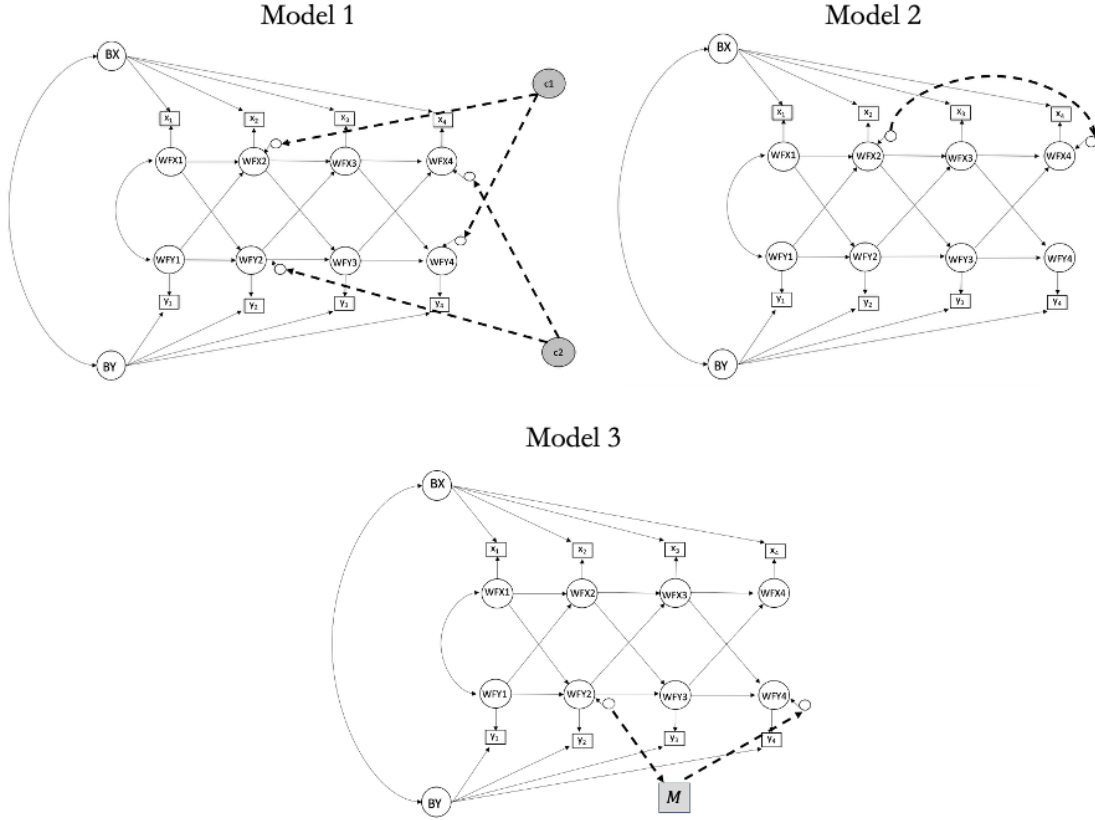
where $\boldsymbol{\Sigma}(\boldsymbol{\theta})$ is the covariance matrix. The vector $\boldsymbol{\varepsilon}_i \sim N(\mathbf{0}, \mathbf{I})$ represents random errors drawn from a standard multivariate normal distribution with zero mean and identity variance. For the parameter values, I set AR parameters β_{xi} and CL parameters γ_{yi} at 0.25 and 0.15, respectively. I use the same parameter values and specifications for the time-varying component of the RI-CLPM across all models to ensure comparability and validate the simulation results. Although parameter choices in simulations can be arbitrary, they do not affect test statistics or fit indices when models are correctly specified.

In the second step, I specify three analysis models that deliberately omit confounders influencing the independent and outcome variables. In the third step, I apply both the LM and Wald tests to detect these omitted confounders and compare their effectiveness. All data generation simulations are performed in R using the `lavaan` package (Rosseel, 2012).

5.1 Population Models

Each population model is a four-wave RI-CLPM with two latent variables, X and Y , measured by single indicators at each time point. The RI-CLPM structure separates within-person fluctuations (for example, deviations from one's mean trajectory) from stable between-person differences. To increase complexity while avoiding overfitting, I use four time points rather than adding more indicators per construct.

Figure 2: Diagrams of Population Models



Note: To simplify the notations, residuals are not shown in the diagrams

6 Population Models & Specification

Figure 2 presents diagrams of three RI-CLPMs that share a common baseline structure but differ in their unmeasured confounding designs. To simplify notation, the remainder of the paper uses WFX to denote the autoregressive path and WFY the cross-lagged path in the within-factor component, while BX and BY represent the between-factor component. This convention makes the statistical output easier to present. As illustrated in Figure 2, each model is based on a four-wave RI-CLPM framework that includes both within-person and between-factor components. For the within-factor component, two sets of latent variables, WFX_i and WFY_i , for $i = 1, 2, \dots, 4$, are specified. Each latent variable is measured by a

single observed indicator, x_i and y_i , respectively. For the between-person component, two latent factors, BX and BY , are introduced to capture stable individual traits. Additionally, BX and BY are allowed to correlate, reflecting the association between stable traits across constructs.

6.1 Model Variants

As shown in Figure 2, **Model 1** introduces two higher-order latent confounders, c_1 and c_2 , representing dynamic confounding between the residuals of WFX_2 and WFY_4 , and between the residuals of WFY_2 and WFX_4 , respectively. For example, in political communication, c_1 could capture unobserved partisan media exposure that simultaneously influences political efficacy and later policy support, while c_2 might reflect unmeasured interpersonal political discussion affecting earlier policy support and later efficacy. By inducing correlated residual variation across time and constructs, these confounders can bias cross-lagged path estimates.

Model 2 imposes a unidirectional direct path from WFX_2 to WFX_4 , representing a case where an earlier latent variable exerts a causal influence on a later one while bypassing intermediate processes. In political behavior terms, this could capture citizens' trust in government at time t directly shaping trust at $t + 2$, without accounting for mediating influences such as media exposure or political events. This specification violates temporal stationarity by assuming the effect remains constant across time, thereby conflating transient causal effects with stable dispositions or prior attitudes.

Model 3 incorporates unmeasured confounding within a mediation framework, where the residual of WFY_2 on the residual of WFY_4 is mediated indirectly through the residual of an unobserved mediator M , which itself is regressed on x_1 . For example, political engagement could mediate the relationship between political efficacy at two time points. Omitting M risks misattributing mediated effects as direct effects, thereby biasing causal interpretations.

In sum, all three models intentionally violate the sequential ignorability assumption. Simulated data from these population models are analyzed using deliberately misspecified

models that omit latent confounders or structural paths, generating the expected model misfit. The simulation examines correlations and regressions among latent variables while fixing factor loadings at 1, ensuring that observed changes reflect only time-varying effects. Because the factor loadings are fixed, between-person correlations and residual variances are excluded. To evaluate generalizability, additional analyses of a five-wave RI-CLPM with two indicators, as well as a conventional CLPM, are presented in the Appendix.

6.2 Baseline Model Specification and Validity

Parameter estimation, model fit, and sensitivity analysis all depend on correct model specification. Before conducting simulations on the three variants, it is crucial to verify that both the baseline population model and the analysis model meet the necessary asymptotic assumptions—that is, how an estimator behaves as the sample size approaches infinity, typically converging in probability to the true parameter, thus providing a theoretical basis for inference when finite-sample behavior is uncertain.

To achieve this, I evaluate the model fit across repeated samples with varying sample sizes. If a model is identified and adequately specified, we expect the model to follow a standard χ^2 distribution, $T_{ML} \sim \chi^2_{df}$, as sample size grows larger, demonstrating asymptotic properties (Bentler & Dijkstra, 1985; Browne, 1984). Accordingly, I use Monte Carlo simulation to generate data from the predefined population models and estimate the corresponding analysis models using the simulated data.

The Monte Carlo simulations in this study were based on the population model. I conducted 500 trials and calculated the average statistics, which are reported in Table 1. I examined the performance of the analysis model by varying the sample sizes from 100 to 10,000. Since the simulated data were normally distributed, the maximum likelihood estimator was sufficient to examine the basic statistical performance and asymptotic properties.

Table 1 presents the average χ^2 test statistics, standard deviations, P -values, rejection rates, and fit indices (NFI, CFI, RMSEA) by sample size. As shown in Table 1, as the sample

Table 1: Simulation results of model fit statistics across sample sizes.

N	χ^2	SD	<i>P</i> -value	Rej Rate	NFI	CFI	RMSEA
100	9.214	4.402	0.490	0.068	0.937	0.959	0.119
200	9.195	4.170	0.486	0.058	0.985	1.000	0.000
300	9.178	4.381	0.491	0.050	0.991	1.000	0.000
500	8.909	4.472	0.513	0.056	0.991	0.998	0.028
800	9.034	4.380	0.501	0.060	0.997	1.000	0.000
1000	9.018	4.140	0.495	0.042	0.999	1.000	0.000
5000	9.138	4.116	0.484	0.040	1.000	1.000	0.000
10000	8.921	4.546	0.513	0.050	1.000	1.000	0.006

size increases, all mean test statistics approach the expected values: $\chi^2 = 9$, $SD = 4.24$, P -value = 0.50, and empirical rejection rate is 0.05. In addition, NFI and CFI approach 1, and RMSEA approaches 0 when the sample sizes are greater than 200. Naturally, with smaller sample sizes, test statistics and fit indices deviate from their expected values—a well-documented issue for the maximum likelihood estimator (Zheng & Bentler, 2021, 2023, 2024). The collective statistical indicators demonstrate that the population and baseline analysis models are well-specified. Based on this baseline model, I will proceed with various analyses.

7 The Two-Stage Process for Confounder Searches

7.1 Stage One: Selection of Testing Parameters

I start with a univariate LM test to identify the top candidate parameters based on their LM χ^2 statistics and EPC values. I select the top 25 parameters from this test but exclude any that violate the following criteria:

- (i) Parameters that contradict temporal ordering (e.g., a variable at time t predicting one at $t - 1$) or conflict with the population model (e.g., LM-suggested correlations between autoregressively linked latent variables or fixed variances). In RI-CLPMs, suggestions linking latent variables to their indicators, which may cause non-identification or convergence problems, are also excluded.

- (ii) Parameters that introduce redundant or meaningless relations, such as correlations between autoregressive and cross-lagged paths, are removed.
- (iii) Parameters with extremely small EPC values are excluded.
- (iv) Finally, I add the remaining candidate parameters one at a time to the analysis model; any parameter that causes convergence or identification issues is removed.

7.2 Stage Two: Wald Test

The Wald test follows, assessing candidate parameters identified by the LM test through a forward stepwise procedure. Each parameter is added individually, and the Wald statistic and P -value are computed at each step. This process continues until all candidates are evaluated, enhancing model parsimony and reducing false positives from overfitting. Ultimately, only parameters with P -values below 0.05 are retained for further analysis.

7.3 Simulation Result

Tables 2–4 present the Monte Carlo simulation results, where the gray-highlighted entries indicate cases in which the confounding variables match those in the population models. In Model 1 (Table 2), the residual correlations $WFX_4 \sim WFY_2$ and $WFX_2 \sim WFY_4$ were successfully identified by the LM chi-square, EPC, and Wald tests, indicating that these variables share common variance driven by a latent confounder. Notably, while the path $WFX_4 \sim WFY_2$ was flagged by the LM chi-square with a strong EPC, its Wald test statistic was small (0.537) and statistically insignificant. In Model 2 (Table 3), the LM test identified several direct effects, including $WFX_4 \sim WFX_2$. However, only this path was validated by the Wald test ($p = 0.019$), consistent with the population model. In Model 3 (Table 4), the LM test and EPC flagged multiple paths, including $WFX_4 \sim M$ and $WFX_4 \sim WFX_2$. Of these, only these two paths were further validated by the Wald test ($p < 0.05$), again aligning with the population model.

Overall, the LM tests effectively detected confounders through large chi-square statistics and EPC values, while the Wald tests confirmed true effects and rejected false ones. More-

over, the estimated AR and CL paths closely matched the population parameters (see Tables A1–A3 in the Appendix). Additional simulations with more complex models—including higher-order latent variables, additional waves, and multiple indicators—are presented in the Appendix and show similarly robust performance.

Table 2: Model 1 (Correlation) Simulation Result

		LM χ^2	EPC	Wald Test	<i>P</i> -value
WFX ₄ $\sim\sim$	WFX ₂	575.299	0.447	12.780	0.000
WFX ₄ \sim	WFX ₂	561.970	0.810	0.537	0.464
WFX ₂ $\sim\sim$	WFX ₄	540.303	0.419	7.874	0.005
WFX ₄ \sim	WFX ₂	515.640	0.764	0.372	0.796
WFX ₄ \sim	X ₂	499.933	0.642	0.481	0.488

Note: I follow the same notation conventions used in `lavaan`, where ‘ \sim ’ denotes a latent variable definition, ‘ \sim ’ indicates a regression relationship, and ‘ $\sim\sim$ ’ represents a covariance or correlation.

Table 3: Model 2 (Direct Effect) Simulation Result

		LM χ^2	EPC	Wald Test	<i>P</i> -value
WFX ₄ \sim	WFX ₂	222.566	1.142	5.547	0.019
WFX ₄ $\sim\sim$	WFX ₃	196.282	-0.110	0.528	0.467
WFX ₄ \sim	Y ₃	190.300	-1.024	1.278	0.258
WFX ₄ \sim	X ₂	172.917	0.458	0.049	0.824

Table 4: Model 3 (Mediation) Simulation Result

	LM	EPC	Wald Test	<i>P</i> -value
WFX ₄ \sim M	285.407	0.742	20.932	0.000
WFX ₄ \sim WFX ₂	183.201	1.578	5.117	0.024
WFX ₄ \sim Y ₃	148.494	1.367	0.546	0.460
WFX ₁ \sim X ₁	143.828	-2.882	0.115	0.735
WFX ₂ $\sim\sim$ WFX ₄	138.537	0.079	0.065	0.799
WFX ₄ \sim Y ₂	132.760	0.447	3.844	0.050
WFX ₄ \sim X ₁	116.008	0.416	0.387	0.534

8 Empirical Application

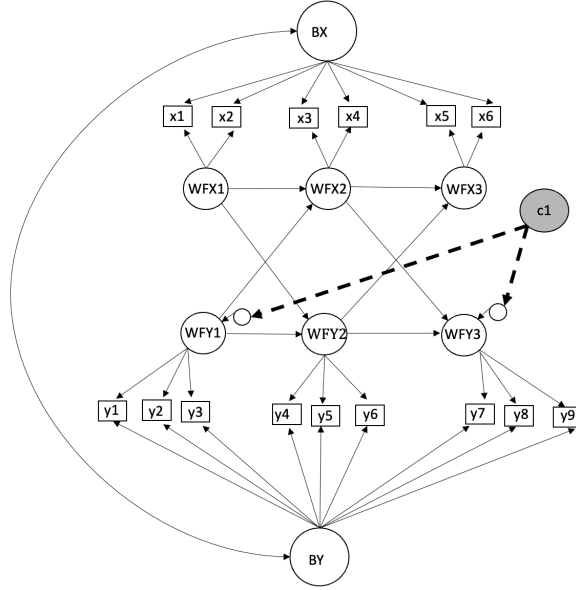
This section presents an empirical example that demonstrates the flexibility of the 2SLW approach and illustrates its application within a RI-CLPM framework. Beyond showcasing the 2SLW method, this example also aims to encourage the broader adoption of RI-CLPM in political behavior research, where its use remains relatively limited.

To this end, I apply the RI-CLPM to data from the Longitudinal Internet Studies for the Social Sciences (LISS) panel—a long-term, internet-based survey of individuals and households in the Netherlands, administered by CentERdata. Building on (Bakker et al., 2021)’s “Reconsidering the Link Between Self-Reported Personality Traits and Political Preferences,” I construct a three-wave panel using data collected in 2008, 2014, and 2020. The RI-CLPM allows us to separate stable individual differences from within-person fluctuations over time as I examine how agreeableness influences attitudes toward immigration.

Agreeableness is measured using two items: (1) “Interested in people”, (2) “I am not interested in other people’s problems” (reverse coded). Immigration attitudes are assessed using three items: (1) “There are too many people of foreign origin or descent in the Netherlands” (2) “Legally residing foreigners should be entitled to the same social security as Dutch citizens”. (3) “It should be made easier to obtain asylum in the Netherlands”. Responses are recorded on a five-point Likert scale ranging from “fully disagree” to “fully agree.”

My analytic strategy is twofold. First, I estimate the causal relationship between agreeableness and immigration attitudes using a standard RI-CLPM. Next, I apply the 2SLW approach to detect potential unmeasured confounders that may bias the estimates. I then compare the goodness-of-fit statistics, fit indices, and the AR and CL coefficient estimates between the baseline model and the improved model using the 2SLW approach.

Figure 3: Diagram of the RI-CLPM



The agreeableness and political attitude items are denoted as X_i and Y_i , respectively, in Figure 3. To examine the effects of agreeableness on immigration attitudes, I construct a series of latent variables, WFX_i and WFY_i , measured by agreeableness and political attitude items across the 2008, 2014, and 2020 waves. The undirected paths among WFX_i and WFY_i represent autoregressive (AR) effects, while the directed paths from WFX_i to WFY_i denote cross-lagged (CL) effects. The dashed lines from the latent variable c_1 to WFY_1 and WFY_3 indicate confounding paths identified by the 2SLW approach.

Table 5: The 2SLW Test Result

			LM χ^2	EPC	Wald Test	P-value
WFY_1	$\sim\sim$	WFY_3	53.615	0.143	15.464	0.000
WFY_3	$=\sim$	Immigrant Benefits (08)	43.627	0.679	1.596	0.207
WFX_1	$\sim\sim$	WFY_3	40.390	-0.244	0.593	0.441
WFY_2	$=\sim$	Immigrant Benefits (08)	38.387	0.969	4.862	0.027

Table 5 presents the results of the LM and Wald tests. The LM test identified four parameters, of which only two were statistically significant according to the Wald test, as

highlighted. Notably, the correlation between WFY_1 and WFY_3 yielded the largest χ^2 value and the highest Wald test statistic, indicating strong statistical significance. These two parameters will be incorporated into the existing model.

Table 6: AR & CL Coefficients of Original and Improved Models

Variable	Original Model			Improved Model			Difference
	Estimate	Std. Err	<i>P</i> -value	Estimate	Std. Err	<i>P</i> -value	Diff
WFX₂ ~							
WFX ₁	0.824	0.031	0.000	0.825	0.027	0.000	0.001
WFY ₁	0.121	0.160	0.450	-0.096	0.016	0.010	-0.217
WFY₂ ~							
WFY ₁	1.585	0.185	0.000	0.977	0.023	0.000	-0.608
WFX ₁	0.047	0.024	0.049	-0.025	0.025	0.026	-0.072
WFX₃ ~							
WFX ₂	0.961	0.030	0.000	0.906	0.029	0.000	-0.055
WFY ₂	0.089	0.081	0.268	0.006	0.015	0.854	-0.083
WFY₃ ~							
WFY ₂	1.015	0.076	0.000	0.861	0.071	0.000	-0.154
WFX ₂	-0.071	0.021	0.001	-0.051	0.081	0.136	0.020
C1 ~							
WFY ₁	0.584						
WFY ₃	0.180	0.143	0.028				
Model Fit							
χ^2	679.509			130.809			-548.700
DF	74			65			-9.000
CFI	0.991			1.000			0.009
NFI	0.990			0.998			0.008
TLI	0.988			1.000			0.012
RMSEA	0.059			0.011			-0.048

Table 6 compares the AR and CL coefficients from the original and improved models. In the original model, the cross-lagged paths from WFX_2 to WFY_1 and from WFY_2 to WFX_1 are statistically significant but run in an unexpected direction. This anomaly likely reflects model misspecification, supported by a poor χ^2 statistic of 679.509 ($df = 74$). The model also exhibits a negative variance estimate, further underscoring the misspecification despite acceptable fit indices.

In sharp contrast, the improved model produces more consistent and theoretically appropriate cross-lagged estimates. While the path from WFX_3 to WFY_2 is not statistically significant, most other parameters are stable and interpretable—that is, they align with find-

ings in the political psychology literature. In particular, stronger agreement with empathetic concern for others is generally associated with reduced support for exclusionary statements (Batson, Chang, Orr, & Rowland, 2002; Simas, Clifford, & Kirland, 2019; Sirin, Valentino, & Villalobos, 2021). Although modest, the latent confounder c_1 —with factor loadings of 0.584 and 0.180, respectively—induces a correlation just above 0.10. Even this small degree of confounding can bias the estimated causal effect and obscure its substantive interpretation.

Importantly, the improved model demonstrates substantially better fit, as reflected by a χ^2 value of 130.809 ($df = 65$). Other fit indices—CFI, NFI, TLI, and RMSEA—also indicate excellent fit. Taken together, Tables 5 and 6 provide strong evidence that the improved model offers a significantly better fit to the data than the original specification. Without identifying the unmeasured confounder, the substantive conclusions about the causal effects—and the arguments built upon them could have been misleading.

9 Discussion & Conclusion

Rigorous investigation of causal effects is fundamental to social and behavioral research, necessitating a diverse set of analytical tools. While panel models are powerful for causal inference with observational data, unobserved confounding continues to pose a significant challenge. This study has introduced the 2SLW approach as a diagnostic tool for identifying potential confounders within the RI-CLPM framework. Through Monte Carlo simulations, I evaluated the method under three scenarios of confounding: distortion of the (1) predictor-outcome association, (2) direct effect, and (3) mediation pathway. I further demonstrated its practical utility through an empirical application. While simulations cannot capture every real-world complexity, results from the RI-CLPM and CLPM demonstrate that the 2SLW approach is effective and scalable. Its design also supports generalization to other SEM-based panel models and extended panel structures.

In light of this, the study offers three key contributions. First, it extends the LM test to

panel causal models, such as the RI-CLPM, enabling a more systematic and less subjective assessment of unmeasured confounding in sensitivity analysis. Second, these methodological advancements improve the reliability of inferences drawn from complex longitudinal panel data by providing stronger diagnostic tools to detect unmeasured confounders in a wide range of applied settings. Third, by improving detection of unmeasured confounding, the approach strengthens causal inference in social and behavioral sciences using SEM panel data.

As others have emphasized, any model modification or sensitivity analysis must be grounded in theory and cross-validation to guard against overfitting. The 2SLW test is no exception. It serves as a data-driven guide for uncovering potential confounding but should be interpreted as exploratory rather than prescriptive. Ultimately, the decision to modify models or add parameters must rest on theoretical justification. While this study focuses on detection, future research could build on this work by integrating formal sensitivity analysis frameworks to estimate the potential impact of unmeasured confounding on causal parameters.

References

- Acharya, A., Blackwell, M., & Sen, M. (2016). Explaining causal findings without bias: Detecting and assessing direct effects [Journal Article]. *American Political Science Review*, *110*, 512-29.
- Bakker, B., Schumacher, G., & Rooduijn, M. (2021). Hot politics? affective responses to political rhetoric [Journal Article]. *American Political Science Review*, *115*(1), 150-164.
- Batson, C. D., Chang, J., Orr, R., & Rowland, J. (2002). Empathy–attitudes–action framework in social psychology [Journal Article]. *Personality and Social Psychology Bulletin*, *28*(12), 1656-1666. doi: <https://doi.org/10.1177/014616702237647>
- Bentler, P. M., & Dijkstra, T. (1985). Efficient estimation via linearization in structural models [Book Section]. In P. R. Kirshnaiah (Ed.), *Multivariate analysis vi* (p. 9-42). Amsterdam: North-Holland.
- Blackwell, M. (2014). A selection bias approach to sensitivity analysis for causal effects. *Political Analysis*, *22*(2), 169–182. doi: 10.1093/pan/mpt006
- Browne, M. (1984). Asymptotically distribution-free methods for the analysis of covariance structures [Journal Article]. *British Journal of Mathematical and Statistical Psychology*, *37*, 62-83. doi: doi:10.1111/bmsp.1984.37.issue-1
- Bullock, J. G., Green, D., & Ha, S. E. (2010). Yes, but what’s the mechanism? (don’t expect an easy answer) [Journal Article]. *Journal of Personality and Social Psychology*, *98*(4), 550-558.
- Chiu, A., Lan, X., Liu, Z., & Xu, Y. (2025). causal panel analysis under parallel trends: Lessons from a large reanalysis study [Journal Article]. *American Political Science Review*, 1-22. doi: <https://doi.org/10.1017/S0003055425000243>
- Chou, C.-P., & Bentler, P. M. (1993). Invariant standardized estimated parameter change for model modification in covariance structure analysis [Journal Article]. *Multivariate Behavioral Research*, *28*(1), 97-110. doi: https://doi.org/10.1207/s15327906mbr2801_6
- Dinesen, P. T., Sonderskov, K. M., Sohlberg, J., & Esaiasson, P. (2022). Close (causally connected) cousins? evidence on the causal relationship between political trust and social trust [Journal Article]. *Public Opinion Quarterly*, *86*(3), 708-721. doi: <https://doi.org/10.1093/poq/nfac027>
- Feldman, S., Panish, A., Weber, C., & Zheng, B. Q. (2025). *Rethinking the cross lagged regression model: Limitations and alternatives in panel analysis* [Conference Paper].
- Goren, P. (2005). Party identification and core political values [Journal Article]. *American Journal of Political Science*, *49*(4), 882-897.
- Hamaker, E. L., Kuiper, R. M., & Grasman, R. P. P. P. (2015). A critique of the cross-lagged panel model [Journal Article]. *Psychological Methods*, *20*, 102-116.
- Harring, J., McNeish, D., & Hancock, G. (2017, December). Using phantom variables in structural equation modeling to assess model sensitivity to external misspecification. *Psychological Methods*, *22*(4), 616–631. doi: 10.1037/met0000103
- Hatemi, P. K., Crabtree, C., & Smith, K. (2019). Ideology justifies morality: Political beliefs predict moral foundations [Journal Article]. *American Journal of Political Science*, *63*(4), 788-806. doi: DOI:10.1111/ajps.12448

- Holland, P. W. (1988). Causal inference, path analysis, and recursive structural equations models [Journal Article]. *Sociological Methodology*, 18, 449-484.
- Imai, K., Keele, L., & Tingley, D. (2010). A general approach to causal mediation analysis [Journal Article]. *Psychol Methods*, 15(4), 309-326.
- Imai, K., Keele, L., Tingley, D., & Yamada, T. (2011). Unpacking the black box of causality: Learning about causal mechanisms from experimental and observational studies [Journal Article]. *American Political Science Review*, 105(4), 765-789.
- Imai, K., & Yamamoto, T. (2013). Identification and sensitivity analysis for multiple causal mechanisms: Revisiting evidence from framing experiments. *Political Analysis*, 21(2), 141-171. doi: 10.1093/pan/mps040
- Lucas, R. (2023). Why the cross-lagged panel model is almost never the right choice [Journal Article]. *Advances in Methods and Practices in Psychological Science*, 6(1), 1-22. doi: <https://doi.org/10.1177/251524592311158>
- Luttig, M. D. (2021). Reconsidering the relationship between authoritarianism and republican support in 2016 and beyond [Journal Article]. *Journal of Politics*, 83(2), 783-787.
- MacCallum, R. C., Roznowski, M., & Nectowitz, L. B. (1992). Model modifications covariance structure analysis: The problem of capitalization on chance [Journal Article]. *Psychological Bulletin*, 111(3), 490-504.
- MacKinnon, D. P. (2008). *Introduction to statistical mediation analysis* [Book]. Routledge.
- MacKinnon, D. P., & Pirlott, A. G. (2015). Statistical approaches for enhancing causal interpretation of the m to y relation in mediation analysis [Journal Article]. *Personality and Social Psychology Review*, 19(1), 30-43.
- Mund, M., Johnson, M. D., & Nestler, S. (2021). Changes in size and interpretation of parameter estimates in within-person models in the presence of time-invariance and time-varying covariate [Journal Article]. *Frontiers in Psychology*. doi: <https://doi.org/10.3389/fpsyg.2021.666928>
- Pearl, J. (2001). Direct and indirect effects [Book Section]. In J. B. . D. Koller (Ed.), *Proceedings of the seventeenth conference on uncertainty in artificial intelligence* (p. 411-420). San Francisco, CA: Morgan Kaufmann Publishers Inc.
- Robins, J. M., & Greenland, S. (1992). Identifiability and exchangeability for direct and indirect effects [Journal Article]. *Epidemiology*, 3(2), 143-155.
- Rosseel, Y. (2012). lavaan: An r package for structural equation modeling [Journal Article]. *Journal of Statistical Software*, 48(2), 1-36.
- Simas, E. N., Clifford, S., & Kirland, J. H. (2019). How empathic concern fuels political polarization [Journal Article]. *American Political Science Review*, 114(1), 258-269. doi: <https://doi.org/10.1017/S0003055419000534>
- Sirin, C. V., Valentino, N., & Villalobos, J. D. (2021). *Seeing us in them social divisions and the politics of group empathy* [Book]. New York: Cambridge University Press. doi: <https://doi.org/10.1017/9781108863254>
- Usami, S. (2021). On the differences between general cross-lagged panel model and random-intercept cross-lagged panel model: Interpretation of cross-lagged parameters and model choice [Journal Article]. *Structural Equation Modeling: A Multidisciplinary Journal*, 28(3), 331-344.
- Usami, S., Murayama, K., & Hamaker, E. L. (2019). A unified framework of longitudinal models to examine reciprocal relations [Journal Article]. *Psychol Methods*, 24(5), 637-

- Yuan, K., & Liu, F. (2021). Which method is more reliable in performing model modification: Lasso regularization or lagrange multiplier test? [Journal Article]. *Structural Equation Modeling: A Multidisciplinary Journal*, 28(1), 69-81.
- Zheng, B. Q., & Bentler, P. (2025). Improved LM test for robust model specification searches in covariance structure analysis: Application in political science research [Journal Article]. *Political Science Research & Methods*, 1-21. doi: doi:10.1017/psrm.2025.27
- Zheng, B. Q., & Bentler, P. M. (2021). Testing mean and covariance structures with reweighted least squares [Journal Article]. *Structural Equation Modeling: A Multidisciplinary Journal*. doi: <https://doi.org/10.1080/10705511.2021.1977649>
- Zheng, B. Q., & Bentler, P. M. (2023). Rgls and rls in covariance structure analysis [Journal Article]. *Structural Equation Modeling: A Multidisciplinary Journal*, 30(2), 234-244. Retrieved from SocArXiv <https://doi.org/10.31235/osf.io/aejgf> doi: <https://doi.org/10.1080/10705511.2022.2117182>
- Zheng, B. Q., & Bentler, P. M. (2024). Enhancing model fit evaluation in sem: Practical tips for optimizing chi-square tests [Journal Article]. *Structural Equation Modeling: A Multidisciplinary Journal*(Advance online publication). doi: <https://www.tandfonline.com/doi/full/10.1080/10705511.2024.2354802>
- Zheng, B. Q., & Valente, M. J. (2023). Evaluation of goodness-of-fit tests in random intercept cross-lagged panel model: Implications for small samples [Journal Article]. *Structural Equation Modeling: A Multidisciplinary Journal*, 30(4), 604-617. doi: <https://doi.org/10.1080/10705511.2022.2149534>

Appendix

The Covariance Matrix of the RI-CLPM

In covariance structure analysis, the RI-CLPM can be expressed through its covariance matrix. Specifically, Equations (5) and (6) can be reformulated in matrix form as follows:

$$\begin{aligned} z_{it} &= \delta_i + \Phi z_{i(t-1)}^* + \eta_i + v_{it}, & (i = 1, \dots, n, t = 1, \dots, T) \\ z_{i1} &= \delta_i + \Psi \eta_i + \epsilon_{i1}, & (i = 1, \dots, n) \end{aligned} \quad (\text{A1})$$

where

$$z_{it} = \begin{bmatrix} x_{it} \\ y_{it} \end{bmatrix}, \quad \Phi = \begin{bmatrix} \beta_x & \gamma_x \\ \beta_y & \gamma_y \end{bmatrix}, \quad \eta_i = \begin{bmatrix} \eta_{xi} \\ \eta_{yi} \end{bmatrix}, \quad v_i = \begin{bmatrix} v_{xit} \\ v_{yit} \end{bmatrix}, \quad \delta_i = \begin{bmatrix} \delta_{xi} \\ \delta_{yi} \end{bmatrix}, \quad (\text{A2})$$

$$\Psi = \begin{bmatrix} \psi_{11} & \psi_{12} \\ \psi_{21} & \psi_{22} \end{bmatrix}, \quad \epsilon_{i0} = \begin{bmatrix} \epsilon_{i0}^y \\ \epsilon_{i0}^x \end{bmatrix}. \quad (\text{A3})$$

Building on the CLPM covariance matrix formulation in Hayakawa (2019), we assume that the largest eigenvalue of Φ is less than 1, ensuring that z_{it} follows a stable process. Using these matrices, we combine Equations (5) and (6) to obtain:

$$Bz_i = \delta_i + J\pi_i + u_i, \quad (\text{A4})$$

where

$$B = \begin{bmatrix} I_2 & 0 & \cdots & 0 \\ -\Phi & I_2 & \cdots & \vdots \\ \vdots & \ddots & \ddots & 0 \\ 0 & 0 & -\Phi & I_2 \end{bmatrix} \quad (\text{A5})$$

$$\Gamma = B^{-1} = \begin{bmatrix} I_2 & 0 & \cdots & 0 \\ \Phi & I_2 & \cdots & \vdots \\ \vdots & \ddots & \ddots & 0 \\ \Phi^{T-1} & 0 & \Phi & I_2 \end{bmatrix} \quad (\text{A6})$$

$$z_i = \begin{bmatrix} z_{i1} \\ z_{i2} \\ \vdots \\ z_{iT} \end{bmatrix}, \quad u_i = \begin{bmatrix} \epsilon_{i1} \\ v_{i2} \\ \vdots \\ v_{iT} \end{bmatrix} \quad (\text{A7})$$

$$J = \begin{bmatrix} 1 & \Psi \\ 0 & I_2 \end{bmatrix}, \quad \pi_i = \begin{bmatrix} \delta_i \\ \eta_i \end{bmatrix} \quad (\text{A8})$$

Thus, we have:

$$z_i = \Gamma(J\pi_i + u_i). \quad (\text{A9})$$

We assume that $\pi_i \sim (0, \Sigma_\pi)$, $v_{it} \sim (0, \Sigma_v)$, $\epsilon_{i0} \sim (0, \Sigma_\epsilon)$, and that δ_i , η_i , v_{it} , and ϵ_{i1} are uncorrelated, independent, and identically distributed. Therefore, the covariance matrix can be written as:

$$\Sigma(\theta) = \Gamma (J\Sigma_{\pi}J' + \Sigma_u) \Gamma', \quad (\text{A10})$$

where

$$\theta = (\Phi, \Psi, \sigma_{\pi}^2, \sigma_v^2, \sigma_{\epsilon}^2)', \quad \Sigma_u = \text{diag}(\sigma_{\epsilon}^2, \sigma_v^2 I_T).$$

Monte Carlo Simulation

The data generation scheme for the simulation follows the covariance matrix of the RI-CLPM described earlier. Specifically, the data are generated as

$$z_i = \Sigma(\theta)^{1/2} \varepsilon_i,$$

where $\Sigma(\theta)$ is the covariance matrix and ε_i follows a standard normal distribution, $\varepsilon_i \sim N(0, 1)$.

For the parameter values, the autoregressive (AR) parameters β_{xi} and cross-lagged (CL) parameters γ_{yi} are set to 0.25 and 0.15, respectively. We use identical parameter values and specifications for the time-varying component of the RI-CLPM across all models to ensure comparability and to validate the simulation results.

Using identical parameter values in the simulation facilitates validation and allows for comparison with existing studies. While the choice of parameter values in simulations can be arbitrary, it does not affect test statistics or fit indices when models are correctly specified. Data generation can be implemented in R using the `lavaan` package.

Five-Wave RI-CLPM with Two Indicators Per Factor

To assess the flexibility of the 2SLW approach, I construct a more complex RI-CLPM featuring five waves of repeated measurements, where each latent factor is measured by two indicators. Additionally, I specify a second-order factor L , which is measured by the factors

η_x and η_y .

Following a similar strategy introduced in the main text, I design three scenarios:

1. The correlation between the two factors is driven by an unobserved latent confounder.
2. The association is modeled as a direct effect between the two factors.
3. The relationship follows a mediation path between two time-varying factors.

Consider two constructs, X and Y , measured at $t = 1, 2$. Each observed score is represented as

$$\begin{aligned} x_{it} &= \delta_{xt} + \eta_{xi} + x_{it}^*, \\ y_{it} &= \delta_{yt} + \eta_{yi} + y_{it}^*, \end{aligned} \tag{A11}$$

with $x_{it}^* \perp y_{is}^*$.

In the cross-lagged panel model (CLPM), the within-person deviations evolve according to

$$\begin{aligned} x_{it}^* &= \beta_x x_{i(t-1)}^* + \gamma_x y_{i(t-1)}^* + v_{xit}, \\ y_{it}^* &= \beta_y y_{i(t-1)}^* + \gamma_y x_{i(t-1)}^* + v_{yit}, \end{aligned} \tag{A12}$$

where the disturbances v_{xit}, v_{yit} have mean zero and are independent of measurement errors.

In the random-intercept CLPM (RI-CLPM), η_{xi} and η_{yi} are treated as time-invariant person-specific components (random intercepts), while the within-person deviations x_{it}^*, y_{it}^* follow the same autoregressive and cross-lagged dynamics:

$$\begin{aligned} x_{it}^* &= \beta_x x_{i(t-1)}^* + \gamma_x y_{i(t-1)}^* + v_{xit}, \\ y_{it}^* &= \beta_y y_{i(t-1)}^* + \gamma_y x_{i(t-1)}^* + v_{yit}. \end{aligned} \tag{A13}$$

Let $\Sigma(\theta)$ denote the model-implied covariance matrix of the observed vector $z_i = (x_{i1}, y_{i1}, x_{i2}, y_{i2})^\top$, expressed as a smooth function of the parameter vector

$$\theta = (\beta_x, \beta_y, \gamma_x, \gamma_y, \dots).$$

Under multivariate normality, the expected Fisher information for any structural parameter $\psi \in \{\beta_x, \beta_y, \gamma_x, \gamma_y\}$ is

$$I(\psi) = \frac{1}{2} \text{tr} \left(\Sigma^{-1} \frac{\partial \Sigma}{\partial \psi} \Sigma^{-1} \frac{\partial \Sigma}{\partial \psi} \right). \quad (\text{A14})$$

Identification requires that the Jacobian

$$J(\theta) = [\text{vec} \left(\frac{\partial \Sigma}{\partial \theta_j} \right) : \theta_j \in \theta] \quad (\text{A15})$$

has full column rank.

Proposition 1 (Weak loadings $\lambda_x \rightarrow 0$ and/or $\lambda_y \rightarrow 0$)

Consider single-indicator CLPM or RI-CLPM, where

$$x_{it} = \delta_{xt} + \eta_{xi} + \lambda_x x_{it}^*, \quad y_{it} = \delta_{yt} + \eta_{yi} + \lambda_y y_{it}^*,$$

with within-person deviations x_{it}^*, y_{it}^* evolving according to the cross-lag dynamics.

For any structural parameter $\psi \in \{\beta_x, \beta_y, \gamma_x, \gamma_y\}$, the derivative of the model-implied covariance matrix scales entrywise with the loadings:

$$\frac{\partial \Sigma}{\partial \psi} = O(\lambda_x \lambda_y). \quad (\text{A17})$$

Hence, the expected Fisher information satisfies

$$I(\psi) = O(\lambda_x^2 \lambda_y^2) \rightarrow 0 \quad (\text{A18})$$

as any loading approaches zero, implying near-zero information and near-nonidentification

of ψ .

Sketch of proof. Observed covariances inherit structural dependencies via the measurement equation:

$$\text{cov}(x_s, y_t) = \lambda_x \lambda_y \text{cov}(x_s^*, y_t^*), \quad (\text{A19})$$

so differentiating w.r.t. ψ introduces the $\lambda_x \lambda_y$ factor. Thus $I(\psi) \sim (\lambda_x \lambda_y)^2$. ■

Proposition 2 (Extremely strong loadings $\lambda_x, \lambda_y \rightarrow 1$)

In single-indicator CLPM/RI-CLPM, when $\lambda_x = \lambda_y \approx 1$ and residuals $v_{xit}, v_{yit} \approx 0$, the columns of $\mathbf{J}(\theta)$ corresponding to measurement and structural parameters become nearly collinear, making the Jacobian ill-conditioned. In RI-CLPM, this includes collinearity between random-intercept variance components and within-person dynamics, yielding weak identification of $(\beta_x, \beta_y, \gamma_x, \gamma_y)$.

Sketch of proof (CLPM). With $\lambda \approx 1$ and negligible measurement error, $x_{it} \approx x_{it}^*$, $y_{it} \approx y_{it}^*$. Changes in Σ from adjusting a structural parameter ψ are nearly indistinguishable from changes caused by latent variance parameters. Thus columns of $\mathbf{J}(\theta)$ are nearly linearly dependent.

Sketch of proof (RI-CLPM). Observed scores are

$$\begin{aligned} x_{it} &= \delta_{xt} + \eta_{xi} + \lambda_x x_{it}^*, \\ y_{it} &= \delta_{yt} + \eta_{yi} + \lambda_y y_{it}^*, \end{aligned} \quad (\text{A20})$$

with $\lambda_x, \lambda_y \approx 1$ and $v_{xit}, v_{yit} \approx 0$. Perturbations in $\text{Var}(\eta_{xi})$ or lag parameters (β_x, γ_x) alter almost the same off-diagonal elements of Σ , yielding an ill-conditioned Jacobian, small Fisher information, and unstable estimates. ■

Corollary (Extremes \Rightarrow instability)

Under either extreme (Proposition 1 or 2), the Fisher information for cross-lag parameters vanishes or the Jacobian is ill-conditioned. Therefore MLEs (or GLS/WLS estimators) of $(\beta_x, \beta_y, \gamma_x, \gamma_y)$ have exploding variance and are highly sensitive to small data perturbations. In practice, this manifests as:

- Cross-lag coefficients that flip sign across specifications or samples;
- Path diagrams whose latent-observed linkages appear “random”;
- Convergence to different local optima depending on starting values.

Practical Identification Conditions

To avoid these degeneracies in CLPM/RI-CLPM:

- Within-person deviations x_{it}^*, y_{it}^* of moderate size with nontrivial residuals v_{xit}, v_{yit} ;
- Multiple indicators per construct per wave (providing additional degrees of freedom);
- Equality constraints on measurement components across waves to fix scale;
- In RI-CLPM, sufficient time points and variation to separately identify between- and within-person components.

These conditions ensure $\mathbf{J}(\theta)$ has full rank and good conditioning, so Fisher information is well-behaved and estimates are stable.

Parameter Estimates based on Table 2, 3, and 4

5-Wave RI-CLPM with 2 Indicators per Construct

In this section, I test the 2SLW approach on the higher-order RI-CLPM, that is, we create an latent variable based on the between-person components. Prior to testing the three

Table A1: Model Estimates

	Estimate	Std. Err	<i>P</i> -value
WFX ₂ ~			
WFX ₁	0.196	0.060	0.001
WFX ₁	0.192	0.056	0.000
WFX ₂ ~			
WFX ₁	0.246	0.059	0.000
WFX ₁	0.192	0.050	0.000
WFX ₃ ~			
WFX ₂	0.235	0.052	0.000
WFX ₂	0.228	0.048	0.000
WFX ₃ ~			
WFX ₂	0.316	0.051	0.000
WFX ₂	0.159	0.045	0.000
WFX ₄ ~			
WFX ₃	0.204	0.041	0.000
WFX ₃	0.229	0.040	0.000
WFX ₄ ~			
WFX ₃	0.150	0.120	0.000
WFX ₃	0.126	0.125	0.002
WFX ₄			
WFX ₂	0.497	0.035	0.000
χ^2	12.954		
DF	8		
CFI	0.998		
NFI	0.995		
TLI	0.994		
RMSEA	0.025		

Table A2: Model Estimates

	Estimate	Std. Err	<i>P</i> -value
WFX ₂ ~			
WFX ₁	0.280	0.051	0.000
WFY ₁	0.216	0.050	0.000
WFY ₂ ~			
WFY ₁	0.216	0.063	0.000
WFX ₁	0.279	0.049	0.000
WFX ₃ ~			
WFX ₂	0.296	0.048	0.000
WFY ₂	0.228	0.045	0.000
WFY ₃ ~			
WFY ₂	0.249	0.054	0.000
WFX ₂	0.274	0.047	0.000
WFX ₄ ~			
WFX ₃	0.336	0.041	0.000
WFY ₃	0.268	0.040	0.000
WFY ₄ ~			
WFY ₃	-0.067	0.435	0.642
WFX ₃	0.514	0.860	0.074
WFY ₂	0.200	0.212	0.005
χ^2	6.723		
DF	7		
CFI	1.00		
NFI	0.997		
TLI	1.00		
RMSEA	0.00		

Table A3: Model Estimates

	Estimate	Std. Err	<i>P</i> -value
WFX ₂ ~			
WFX ₁	0.125	0.071	0.000
WFY ₁	0.115	0.065	0.000
WFY ₂ ~			
WFY ₁	0.091	0.070	0.004
WFX ₁	0.165	0.070	0.000
WFX ₃ ~			
WFX ₂	0.472	0.015	0.000
WFY ₂	0.407	0.015	0.000
WFY ₃ ~			
WFY ₂	0.411	0.015	0.000
WFX ₂	0.482	0.014	0.000
WFX ₄ ~			
WFX ₃	0.125	0.066	0.000
WFY ₃	0.192	0.068	0.000
WFY ₄ ~			
WFY ₃	0.172	0.065	0.000
WFX ₃	0.138	0.060	0.000
Covariances			
WFX ₄ WFY ₂	0.803	0.022	0.000
WFX ₂ WFY ₄	0.810	0.023	0.000
χ^2	5.753		
DF	7		
CFI	1.00		
NFI	0.999		
TLI	1.00		
RMSEA	0.00		

scenarios, I create a baseline model, which is based on Figure A1 but without the dashed lines. As emphasized by previous studies, SEM-based panel models, including RI-CLPM, CLPM, latent growth models, etc., are based on parametric and asymptotic properties. That is, they are linear and follow a distribution. Asymptotic properties refer to how an estimator or test behaves as the sample size approaches infinity, with key features such as consistency—where the estimator converges in probability to the true parameter—providing theoretical justification for inference when finite-sample behavior is uncertain or complex.

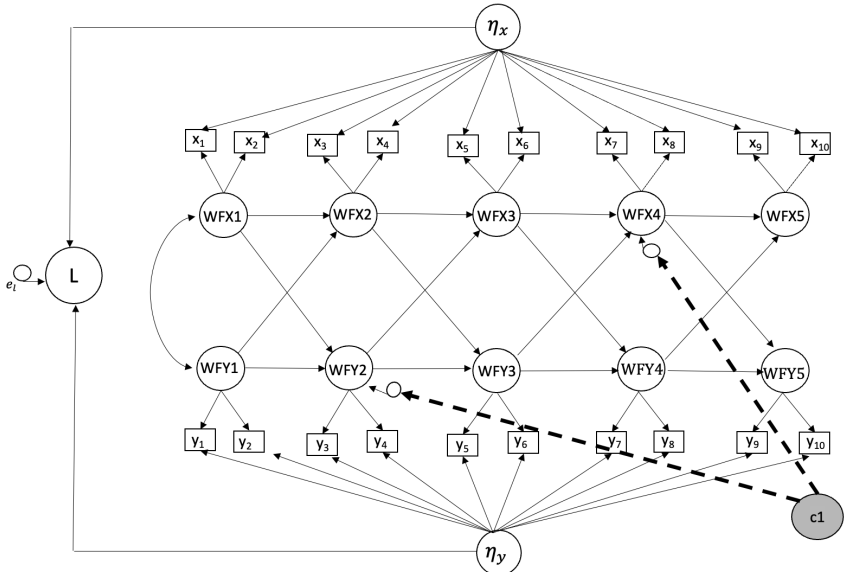


Figure A1: 5-Wave RI-CLPM with 2 Indicators (Correlation)

Table A4: Monte Carlo and Asymptotic Results for 5-Wave RI-CLPM

N	LM χ^2	SD	<i>P</i> -value	Rej Rate	NFI	CFI	RMSEA
100	186.332	19.895	0.273	0.215	0.841	0.993	0.020
200	177.391	18.738	0.389	0.101	0.922	1.000	0.000
300	175.550	18.554	0.415	0.078	0.945	1.000	0.000
500	172.176	19.222	0.472	0.070	0.960	0.997	0.011
800	172.169	19.271	0.469	0.068	0.974	0.997	0.012
1000	171.764	17.909	0.476	0.066	0.982	1.000	0.000
5000	171.068	18.024	0.490	0.062	0.996	1.000	0.003
10000	169.742	18.433	0.505	0.050	0.998	1.000	0.000

Note: Theoretically expected mean $\chi^2 = 170$, SD = 18.44, *P*-value = 0.5, rejection rate = 0.05.

Table A5: Test Result for 5-Wave RI-CLPM with 2 Indicators (Correlation)

Parameter	Operator	Predictor	LM	EPC	Wald Test	<i>P</i> -value
WFX ₄	~~	WFX ₂	42.594	0.468	9.597	0.002
WFX ₅	~	WFX ₂	33.129	-0.337	1.839	0.175
WFX ₅	~~	WFX ₂	29.012	-0.374	0.676	0.411
WFX ₄	~	WFX ₁	12.763	-0.268	0.111	0.739
WFX ₄	=~	Y ₂₂	8.778	0.141	0.616	0.433
WFX ₁	~~	WFX ₄	8.008	-0.236	0.010	0.920
WFX ₃	=~	X ₃₂	6.658	0.155	3.516	0.061
X ₃₁	~~	Y ₃₂	6.190	-0.122	2.493	0.114

Figure A1 illustrates a hypothetical scenario where a latent confounder, c_1 , affects the residuals of WFX₄ and WFX₂. Using this specification, I generate a population model. I then estimate an analysis model that omits c_1 and its direct effects on the residuals of WFX₄

and WFY_2 .

If the 2SLW approach functions as intended, it should detect the residual correlation between WFX_4 and WFY_2 induced by the omitted confounder. However, this relationship is not always straightforward. In some cases, the LM test may identify a correlation or directional effect between WFX_4 and WFY_2 that appears statistically significant, even when the underlying causal structure is more complex.

The final selection between these specifications can be guided by overall model fit, comparing a model that includes a direct effect to one that specifies a correlation between the factors. Naturally, including the true confounder(s) in the model will improve the χ^2 test statistic and overall fit indices.

Table A4 shows that the average of the χ^2 test statistics approaches the expected value of 170 when the sample size is sufficiently large. The standard deviation of the χ^2 test statistics, the average P -value, and the rejection rate are also close to their expected values of 18.44, 0.5, and 0.05, respectively. In addition, the CFI, NFI, and TLI are close to 1, while the RMSEA is near 0. Taken together, these results suggest that the model is well specified.

Table A5 shows the 2SLW results, as we can see that it successfully identified the correlation between WFX_4 and WFY_2 .

Table A6: AR & CL Effects – 5-Wave RI-CLPM (Correlation)

Parameter	Estimate	Std. Err	P-value
WFX₂ ~			
WFX ₁	0.354	0.063	0.000
WFX ₁	0.123	0.062	0.026
WFY₂ ~			
WFY ₁	0.175	0.067	0.003
WFX ₁	0.017	0.066	0.788
WFX₃ ~			
WFX ₂	0.253	0.054	0.000
WFY ₂	0.152	0.054	0.022
WFY₃ ~			
WFY ₂	0.239	0.053	0.000
WFX ₂	0.249	0.052	0.000
WFX₄ ~			
WFX ₃	0.003	0.107	0.975
WFY ₃	0.106	0.076	0.107
WFY₄ ~			
WFY ₃	0.143	0.072	0.054
WFX ₃	0.195	0.084	0.013
WFX₅ ~			
WFX ₄	0.225	0.056	0.001
WFY ₄	0.162	0.072	0.020
WFY₅ ~			
WFY ₄	0.140	0.074	0.084
WFX ₄	0.273	0.050	0.000

Model Fit

χ^2 155.733₄₂

DF 169

CFI 1.000

Figure A2: 5-Wave RI-CLPM with 2 Indicators (Direct Effect)

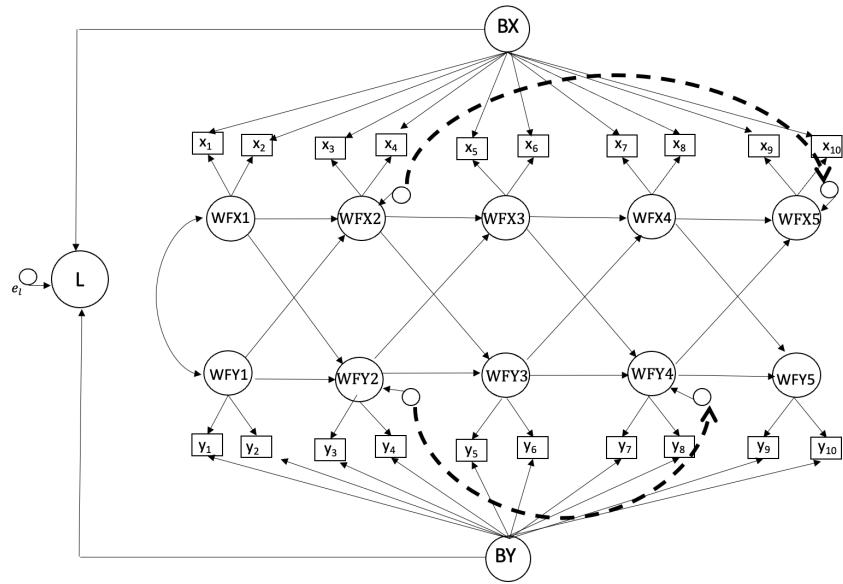


Table A7: Test Result for 5-Wave RI-CLPM with 2 Indicators (Direct Effect)

Parameter	Operator	Predictor	LM χ^2	EPC	Wald Test	<i>P</i> -value
WFX ₅	~	WFX ₂	113.635	1.022	209.231	0.000
WFX ₂	~~	WFX ₅	95.532	0.690	2.881	0.090
WFX ₄	~	WFX ₂	94.187	-0.827	0.970	0.325
WFX ₂	~~	WFX ₄	79.406	-0.554	11.150	0.001
WFY ₄	~	WFY ₂	29.105	0.867	0.413	0.520
WFY ₂	~~	WFY ₄	25.333	0.441	0.413	0.520

Table A8: AR & CL Effects – 5-Wave RI-CLPM (Direct Effect)

Parameter	Estimate	Std. Err	<i>P</i> -value
WFX₂ ~			
WFX ₁	0.407	0.062	0.000
WFX ₁	0.226	0.069	0.000
WFY₂ ~			
WFY ₁	0.155	0.069	0.037
WFX ₁	0.281	0.059	0.000
WFX₃ ~			
WFX ₂	0.262	0.070	0.001
WFY ₂	0.264	0.080	0.000
WFY₃ ~			
WFY ₂	0.126	0.083	0.134
WFX ₂	0.092	0.055	0.201
WFX₄ ~			
WFX ₃	0.272	0.118	0.057
WFY ₃	-0.003	0.097	0.980
WFY₄ ~			
WFY ₃	0.118	0.069	0.038
WFX ₃	0.200	0.062	0.001
WFX₅ ~			
WFX ₄	0.131	0.077	0.011
WFY ₄	0.177	0.052	0.000
WFY₅ ~			
WFY ₄	0.184	0.063	0.021
WFX ₄	-0.020	0.115	0.860
WFX₅ ~			
WFX ₂	0.625	0.047	0.000
WFY₄ ~			
WFY ₂	0.423	0.078	0.000

Table A9: Test Result for 5-Wave RI-CLPM with 2 Indicators (Mediation)

Parameter	Operator	Predictor	LM χ^2	EPC	Wald Test	<i>P</i> -value
WFX ₄	~	WFX ₂	24.742	0.747	72.181	0.000
WFX ₂	~~	WFX ₅	22.761	-0.302	2.520	0.112
WFX ₅	~	WFX ₂	21.493	-0.461	0.075	0.784
WFX ₁	~~	WFX ₄	12.717	0.248	61.918	0.000
x ₃₁	~~	x ₃₂	9.273	5.633	0.017	0.898

Table A10: AR & CL Effects – 5-Wave RI-CLPM (Mediation)

Parameter	Estimate	Std. Err	<i>P</i> -value
WFX ₂ ~			
WFX ₁	0.085	0.081	0.275
WFX ₁	0.187	0.072	0.010
WFX ₂ ~			
WFX ₁	0.248	0.072	0.000
WFX ₁	0.065	0.072	0.325
WFX ₃ ~			
WFX ₂	0.145	0.074	0.063
WFX ₂	0.120	0.061	0.079
WFX ₃ ~			
WFX ₂	0.270	0.065	0.000
WFX ₂	0.210	0.066	0.001
WFX ₄ ~			
WFX ₃	0.042	0.073	0.369
WFX ₃	0.041	0.057	0.333
WFX ₄ ~			
WFX ₃	0.241	0.070	0.001
WFX ₃	0.086	0.075	0.216
WFX ₅ ~			
WFX ₄	0.189	0.043	0.002
WFX ₄	0.130	0.068	0.055
WFX ₅ ~			
WFX ₄	0.167	0.080	0.037
WFX ₄	0.242	0.037	0.000
WFX ₄ ~			
M	0.561	0.039	0.000
WFX ₂	0.455	0.071	0.000
M ~			
x ₁₁	0.629	0.019	0.000
χ^2	200.318		
DF	187		
CFI	0.999		
NFI	0.981		
TLI	0.998		
RMSEA	0.008		

Note: All coefficients are standardized.

Cross-Lagged Panel Model (CLPM)

I construct a CLPM model to test the 2SLW approach, following the same simulation procedure described earlier in the paper. In the population model, AR coefficients are set to 0.5, CL coefficients to 0.2, and residual correlations within time points to 0.3. Before proceeding with the analysis, it is essential to validate the baseline CLPM population model. This baseline model serves as the foundation for generating variants to test the 2SLW approach. The baseline structure, excluding the dashed lines, is illustrated in Figure A3.

Table A11: Monte Carlo and Asymptotic Results for CLPM

N	χ^2	SD	<i>P</i> -value	Rej Rate	NFI	CFI	RMSEA
100	13.060	5.332	0.444	0.076	0.981	1.000	0.000
200	12.640	5.035	0.463	0.060	0.995	1.000	0.000
300	11.923	4.850	0.501	0.046	0.994	1.000	0.000
500	12.171	5.076	0.494	0.058	0.997	1.000	0.000
800	11.746	4.906	0.521	0.064	0.995	0.998	0.027
1000	12.000	5.085	0.501	0.058	0.997	1.000	0.012
5000	11.794	4.982	0.513	0.036	1.000	1.000	0.000
10000	12.130	4.794	0.490	0.036	1.000	1.000	0.006

Note: Theoretically expected mean $\chi^2 = 12$, SD= 4.898, *P*-value=0.5, rejection rate=0.05.

As shown in Table A11, the χ^2 test statistics are close to the degrees of freedom ($df = 12$), with a standard deviation of 4.898, an average *P*-value of 0.05, and an average rejection rate of 0.05. The fit indices, NFI and CFI, are near 1.0, while RMSEA approaches 0. These results indicate that the population model adheres to asymptotic properties and it is well specified.

Figure A4: Diagram of CLPM (Correlation)

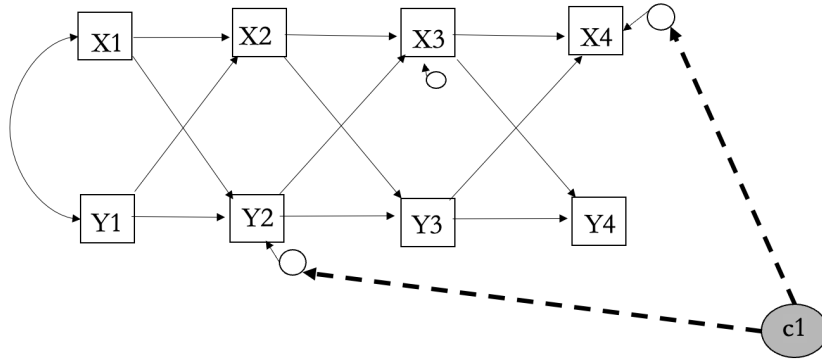


Table A12: Test Result for CLPM (Correlation)

	LM	EPC	Wald Test	<i>P</i> -value
$X_4 \sim Y_2$	282.919	0.426	217.073	0.000
$X_4 \sim Y_3$	210.982	-0.440	0.507	0.476
$X_4 \sim Y_2$	161.480	0.411	0.282	0.595
$X_2 \sim X_4$	64.346	-0.140	0.695	0.405
$Y_2 \sim Y_4$	60.740	-0.149	0.021	0.884
$Y_4 \sim Y_2$	37.786	-0.150	0.240	0.624
$X_2 \sim Y_4$	10.857	0.043	0.140	0.708
$Y_4 \sim Y_1$	3.925	0.042	3.940	0.047

Table A12 shows that the 2SLW approach successfully identified the correlation between X_4 and Y_2 . However, it also flagged a correlation between Y_4 and Y_1 , which was only marginally significant. After including this parameter in the model, the coefficient remained statistically insignificant, suggesting that—despite being identified by the 2SLW—it lacks substantive meaning. Therefore, I decided to exclude it from the final model.

Table A13 shows that after including the confounder, the model became well specified. The autoregressive and cross-lagged coefficient estimates closely matched those of the population model. Moreover, the χ^2 test statistic was 6.826 with 11 degrees of freedom, and the

Table A13: AR & CL Effects for CLPM (Correlation)

	Estimate	Std. Err	<i>P</i> -value
$X_2 \sim X_1$	0.591	0.022	0.000
$X_3 \sim X_2$	0.483	0.030	0.000
$X_4 \sim X_3$	0.407	0.042	0.000
$Y_2 \sim Y_1$	0.391	0.027	0.000
$Y_3 \sim Y_2$	0.550	0.024	0.000
$Y_4 \sim Y_3$	0.504	0.035	0.000
$Y_2 \sim X_1$	0.191	0.027	0.000
$Y_3 \sim X_2$	0.184	0.029	0.000
$Y_4 \sim X_3$	0.193	0.035	0.000
$X_2 \sim Y_1$	0.160	0.023	0.000
$X_3 \sim Y_2$	0.250	0.025	0.000
$X_4 \sim Y_3$	0.124	0.044	0.000
$X_4 \sim Y_2$	0.471	0.029	0.000
Model Fit			
χ^2	6.826		
DF	11		
CFI	1.000		
NFI	0.998		
TLI	1.002		
RMSEA	0.000		

CFI, NFI, and TLI were all close to 1.00, with an RMSEA of zero. Together, these results confirm that the 2SLW approach successfully identified the unmeasured confounder.

Cross-Lagged Panel Model—Direct Effect

In Figure A5, I create two direct effects in the CLPM, connecting X_2 and X_4 , as well as Y_1 and Y_3 . Table A8 presents the 2SLW results, which efficiently identified the unmeasured confounders: the LM test flagged potential parameters, and the Wald test confirmed the correct ones.

Figure A5: Diagram of CLPM (Direct Effect)

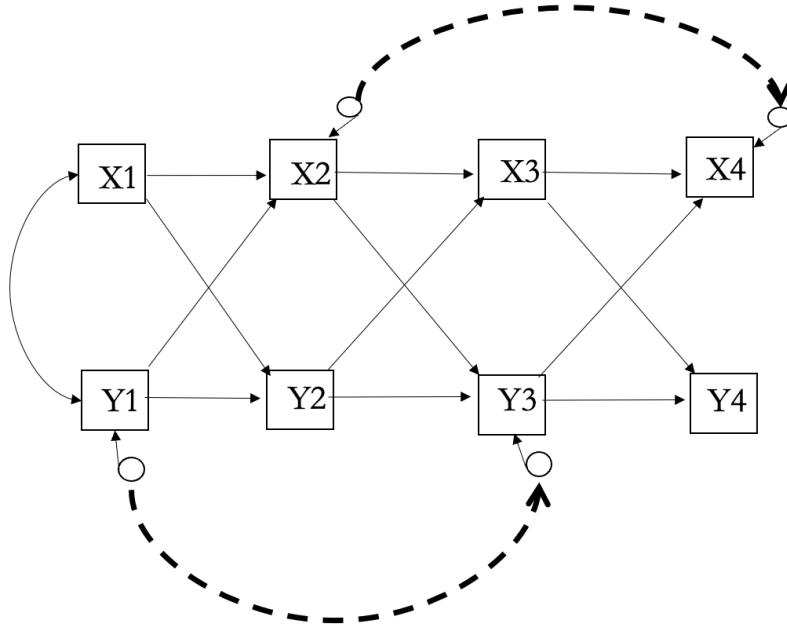


Table A14: Test Result for CLPM (Direct Effect)

Path	LM	EPC	Wald Test	<i>P</i> -value
$Y_3 \sim Y_1$	477.388	0.639	914.578	0.000
$Y_3 \sim\sim Y_1$	451.092	0.590	0.171	0.679
$X_4 \sim X_2$	377.715	0.653	605.803	0.000
$X_2 \sim\sim X_4$	174.765	0.187	0.600	0.439
$X_3 \sim Y_1$	99.274	-0.239	0.418	0.518
$X_3 \sim\sim Y_1$	96.026	-0.224	0.351	0.554
$Y_4 \sim X_2$	94.751	-0.276	0.333	0.564
$X_4 \sim X_1$	77.505	0.223	0.014	0.905
$X_4 \sim\sim X_1$	77.042	0.196	0.318	0.573
$Y_4 \sim\sim X_1$	23.087	-0.091	0.306	0.580
$Y_4 \sim Y_2$	22.706	-0.157	0.534	0.465

Table A15: AR & CL Effects for CLPM (Direct Effect)

Path	Estimate	Std. Err	<i>P</i> -value
$X_2 \sim X_1$	0.536	0.024	0.000
$X_3 \sim X_2$	0.522	0.033	0.000
$X_4 \sim X_3$	0.366	0.035	0.000
$Y_2 \sim Y_1$	0.535	0.022	0.000
$Y_3 \sim Y_2$	0.354	0.036	0.000
$Y_4 \sim Y_3$	0.607	0.023	0.000
$Y_2 \sim X_1$	0.190	0.023	0.000
$Y_3 \sim X_2$	0.151	0.031	0.000
$Y_4 \sim X_3$	0.159	0.032	0.000
$X_2 \sim Y_1$	0.204	0.023	0.000
$X_3 \sim Y_2$	0.185	0.034	0.000
$X_4 \sim Y_3$	0.153	0.024	0.000
$Y_3 \sim Y_1$	0.500	0.021	0.000
$X_4 \sim X_2$	0.443	0.027	0.000
Model Fit			
χ^2	3.546		
DF	10		
CFI	1.000		
NFI	0.999		
TLI	1.003		
RMSEA	0.000		

Note: All coefficients are standardized.

Table A15 shows that, after incorporating the suggested unmeasured confounders into

the original model, the χ^2 statistic and fit indices indicate excellent fit. Moreover, the AR and CL coefficients closely match those of the population model.

Cross-Lagged Panel Model—Mediation

To test whether the 2SLW approach can identify a mediation path in the CLPM, I specify the model shown in Figure A6, where M serves as the mediator between X_2 and X_4 . The model includes both the direct effect of X_2 on X_4 , controlling for M , and the indirect effect of X_2 on X_4 through M . To construct this mediation structure, I regress M on x_1 , inducing a high correlation between the two.

Table A16 shows that the 2SLW approach identifies four unmeasured confounders. Specifically, X_4 is predicted by both X_2 and M , as well as by x_1 . Because M is regressed on x_1 , their LM test statistics are identical, and the Wald test reveals a multicollinearity issue between them. Therefore, we disregard the path $Y_4 \sim x_1$ in subsequent analyses. Additionally, the 2SLW approach identifies $Y_4 \sim x_1$ as statistically significant.

To validate this suggested confounder, I include it in the revised model. As shown in Table A16, the coefficient for $Y_4 \sim x_1$ is small and not statistically significant, indicating it carries little explanatory value. I recommend excluding this parameter from further analysis.

Figure A6: Diagram of CLPM (Mediation)

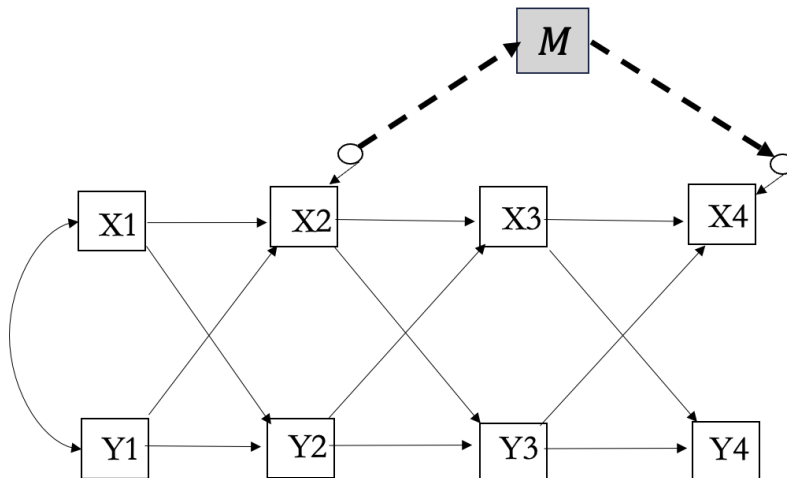


Table A16: AR & CL Effects for CLPM (Mediation)

Path	Estimate	Std. Err	<i>P</i> -value
$X_2 \sim X_1$	0.548	0.023	0.000
$X_3 \sim X_2$	0.507	0.033	0.000
$X_4 \sim X_3$	0.284	0.038	0.000
$Y_2 \sim Y_1$	0.521	0.023	0.000
$Y_3 \sim Y_2$	0.489	0.035	0.000
$Y_4 \sim Y_3$	0.528	0.035	0.000
$Y_2 \sim X_1$	0.237	0.023	0.000
$Y_3 \sim X_2$	0.204	0.034	0.000
$Y_4 \sim X_3$	0.125	0.035	0.001
$X_2 \sim Y_1$	0.194	0.023	0.000
$X_3 \sim Y_2$	0.191	0.034	0.000
$X_4 \sim Y_3$	0.155	0.035	0.000
$c_1 \sim x_1$	0.923	0.007	0.000
$X_4 \sim X_2$	0.450	0.026	0.000
M	0.314	0.038	0.000
$Y_4 \sim x_1$	0.042	0.020	0.074

Model Fit

χ^2	28.972
DF	26
CFI	1.000
NFI	0.996
TLI	0.999
RMSEA	0.011

Note: All coefficients are standardized.

Table A16 shows that the model is well specified, as indicated by a χ^2 statistic of 28.972 with $df = 26$. All fit indices (CFI, NFI, TLI, and RMSEA) fall within acceptable ranges. Moreover, all AR and CL coefficients are statistically significant, except for the path from X1 to Y4. Additionally, all parameter estimates are close to those of the population model, indicating that the 2SLW approach successfully identified the unmeasured mediator.